For the Metallomics special issue in memory of Silvia Atrian - Revised version

The type 4 metallothionein from *Brassica napus* seeds folds in a metal-dependent fashion and favours zinc over other metals

Agnieszka Mierek-Adamska[ab], Grażyna B. Dąbrowska[a], Claudia A. Blindauer[*b]

[a] Department of Genetics, Faculty of Biology and Environmental Protection, Nicolaus Copernicus University, Lwowska 1, 87-100 Toruń, Poland
[b] Department of Chemistry, University of Warwick, Coventry CV4 7AL, UK

To whom correspondence should be addressed:
[*]Claudia A. Blindauer
e-mail: C.Blindauer@warwick.ac.uk
tel. +44 (0)2476 528264

Abstract

The problem of handling zinc in the cell is of great importance because zinc is an indispensable micronutrient involved in most physiological processes in all living organisms. Moreover, our understanding of mechanisms governing the discrimination between micronutrients and toxic metals on the level of individual proteins to the whole-organism level is incomplete. Metallothioneins are able to bind heavy metal ions, and roles in zinc homeostasis have been proposed. Here, we have studied the *in vitro* and *in vivo* metal-binding abilities of *Brassica napus* type 4 metallothionein (BnMT4) and its expression in germinating seeds in response to metal treatment. Our studies on the regulation of MT4 expression by metals at early stages of ontogenic development revealed for the first time that the mRNA levels of *BnMT4* were elevated in response to cadmium and zinc. Given this unexpected metalloregulation, and the dramatic differences in protein folding as detected by ^{1}H NMR spectroscopy, we suggest that the BnMT4 protein may not only have a role in zinc homeostasis in early ontogenesis, but also the potential to discriminate between zinc and cadmium, perhaps via differential recognition of Cd- and Zn-complexes by cellular components involved in protein turnover.

Significance to metallomics

Correctly populating every metalloprotein with the right metal in the cell is indisputably crucial to health and survival of all organisms. However, our understanding of the molecular mechanisms underlying discrimination between metals in biological systems is incomplete. Our research considers *in vitro* properties of copper-, cadmium- and zinc-metallothionein complexes combined with *in vivo* analysis. Therefore, it provides not only evidence for metal-dependent protein folding but also insight into the possible role of this process in the cell.

Key words

cadmium, E_c protein, electrospray ionisation mass spectrometry, germination, heavy metals, metallothioneins, rapeseed, seeds, zinc

Abbreviations

ESI-MS – electrospray ionisation mass spectrometry

ICP-OES - inductively-coupled plasma optical emission spectroscopy

FPLC – fast protein liquid chromatography

MTs – metallothioneins

MRE - metal response element

Introduction

A significant part of agricultural land is deficient in zinc[1] and it is estimated that over 30% of the world's population is at risk of zinc malnutrition (www.who.org). The effects of Zn deficiency are profound and all-encompassing, because a given proteome of a higher eukaryote consists to *ca*. 10% of zinc-requiring proteins.[2] In animals and man, almost all systems including immune, central nervous and reproductive systems are affected by insufficient zinc intake.[3] In plants, more than 1200 proteins contain zinc including carbonic anhydrase critical for carbon fixation,[4] and therefore zinc deficiency leads to reduced growth, low photosynthetic efficiency, delay in flowering and decreased crop yields.[5] The total amount of zinc accumulated in seeds has a significant impact on early vegetative growth of wheat seedlings[6] and the size and number of produced grains.[7] Also seed zinc content of *Brassica napus* (rapeseed, canola) affects the growth of seedlings and their zinc uptake, especially under zinc deficiency conditions.[8] In wheat, barley and rice, Zn is localised mainly in the embryo, but also in the aleurone layer and endosperm,[9-12] whereas in endospermless *B. napus* seeds, zinc is accumulated mainly in cotyledons. During germination, its amount increases in the radicle, the most intensively growing tissue.[13] The detailed chemical speciation of zinc in seeds remains to be determined.[14] Recent work revealed that phytate is not the main storage form of zinc in rice seeds, since the distribution pattern of Zn differs from that of phosphorus.[11] Similarly, in barley grains zinc seems to be bound to peptides and/or proteins rather than to phytate. These peptides/proteins remain to be identified; however, a part of accumulated Zn is coordinated by proteins containing thiol groups.[15]

Type 4 metallothioneins (MTs) are thiol-rich proteins present in abundant quantities in seeds of both mono- and dicotyledons, and their role as zinc/metal chelators has been proposed.[16,17] They belong to a large super-family of low-molecular-weight (<10 kDa), cysteine-rich proteins able to bind heavy metal ions with d^{10} configuration, and are found throughout all kingdoms of life.[18,19] The first plant metallothionein (pMT) discovered was early cysteine-labelled (E_c) protein isolated in a Zn-bound form from wheat germs.[20] Plant MTs are much more diverse in terms of length, number and arrangement of Cys residues than MTs from species of other kingdoms and hence, they were classified into four main types, type 1-3 and type 4, also known as type E_c.[21-23] The expression of pMTs is affected by many endo- and exogenous stimuli including metal ions, reactive oxygen species, phytohormones, or the

presence of microorganisms. Moreover, pMT expression is dependent on the phase of plant development, is tissue-specific and varies depending on the type of pMT.[23-26] pMT4 expression in most angio- and gymnosperms is restricted to developing and mature seed and declines rapidly after the start of germination.[17,27-31] The most likely main function of pMT4s is storage of zinc in seeds and its distribution to nascent Zn-requiring proteins during germination.[17,32] However, pMT4 is also expressed in young and mature leaves and sheaths of rice[33] and in leaves of the desiccation-tolerant resurrection plant *Xerophyta humilis*.[34] Here, the expression of pMT4 is dehydration-upregulated and rehydration-downregulated which may imply that pMT4 has physiological functions beyond micronutrient homeostasis.

Most studies concerning pMTs have been restricted to genes and their mRNA and thus, knowledge about structural and functional properties of pMT proteins is limited, although a few labs including that of Silvia Atrian have begun to remedy this lack of knowledge. One reason for scarce data is a high tendency for proteolytic degradation of pMTs during isolation, especially from native sources.[35] So far, the only pMT isolated directly from plant material in amounts sufficient for further characterisation is the wheat E_c protein.[20,36] Equally, the solution NMR structures of its two domains, from recombinantly expressed protein, remain the only 3D structures available for pMTs.[37,38] pMT4s comprise three cysteine-rich sections separated by two short Cys-free stretches, thus differing from other types of pMTs, which have Cys residues grouped into two regions, separated by a Cys-free stretch of variable length. Wheat E_c, irrespective of whether isolated from wheat embryos[20,36] or produced recombinantly in *E. coli*,[39] binds predominantly six zinc ions in two domains: the N-terminal γ-domain containing a Zn_2Cys_6 cluster, and a C-terminal domain with 11 Cys and 2 His residues that together bind 4 Zn(II) ions. NMR studies revealed that this domain contains a mononuclear $ZnCys_2His_2$ site; this site and the γ-domain Zn_2Cys_6 cluster are unprecedented features for MTs.[37,38,40]

The current report focuses on the dicot rapeseed, one of the most widely cultivated oil-plants. Its seeds are used for production of high-value food oil, biofuels and also protein-rich by-products for animal feed. Only a few studies regarding rapeseed MTs have been published so far;[30,41-45] all of these were limited to the mRNA level and only two of them concern also a type 4 MT.[30,45]

Agricultural land might easily be contaminated with cadmium through fertilization with cadmium-rich phosphate fertilizers. Cadmium and zinc share similar physical and chemical properties[46] and toxic effects of cadmium on plants are mainly caused by the replacement of essential metals by cadmium from a variety of biological ligands.[47] The folding of wheat E_c protein depends on the bound metal and has been hypothesised to promote selective accumulation of essential zinc in the developing embryo over toxic cadmium.[48] Inspired by the postulated role for pMT4s in metal discrimination and reports on elevated cadmium accumulation in rapeseed,[49] we have studied *BnMT4* expression in *B. napus*, metal-binding properties and protein folding of metallated recombinant BnMT4 protein, and its ability to confer tolerance to Zn, Cd, and Cu when expressed heterologously in *E. coli*.

Experimental

Plant materials and heavy metal ion treatment

Seeds from *B. napus* winter variety Kronos (AgroBras, Poland) were surface-sterilized in a mixture of 30% hydrogen peroxide and 96% ethanol in a 1:1 ratio (*v/v*) for 5 min and rinsed with sterile water for 30 min. The seeds were placed in Petri dishes on sterile filter paper moistened with 6 mL of sterile water (control) or 6 mL of 500 µM $ZnSO_4$, 250 µM $CuSO_4$ or 250 µM $CdSO_4$, respectively. Seeds were incubated in darkness at 26°C and material was collected after 3, 12, 24 and 48 hours after the start of seed imbibition, frozen in liquid nitrogen, and stored at -80°C.

Total RNA isolation and reverse transcription reaction

Total RNA isolation was performed using TRI-Reagent (Sigma-Aldrich, Poland) according to manufacturer's protocol. The integrity of RNA was checked on 1% agarose gels in TAE (Tris/acetate/EDTA, pH 8.3) buffer with ethidium bromide (EtBr).

For the reverse transcription (RT) reaction, the following mixture of a total volume of 14.5 µL was prepared: 3 µg of total RNA, 0.5 µg of oligo$(dT)_{18}$ primer and 1 µL of 10 mM dNTPs. The mixture was incubated at 65°C for 5 min, and then at 0°C for 2 min. After that 40 U of RNase inhibitor, 4 µL of 5x RT Buffer and 200 U of RevertAid™ Premium Reverse Transcriptase (Thermo Scientific, MA, USA) was added. The reaction was performed at 50°C for 30 min, and then stopped at 85°C for 5 min. The cDNA was stored at -20°C.

BnMT4 expression analysis

A *BnMT4* cDNA clone was obtained as reported previously (GenBank accession number JX103202.1).[30] Semi-quantitative RT-PCR (sqRT-PCR) forward and reverse primers specific for *BnMT4* were as follows: 5'-GAAGAAAAAGAGCGAGGTAAAA-3' and 5'-CACCCATTCCCAAGGTATGT-3'. The 5S rRNA (*Bn5S*) transcript level was used as internal standard: forward primer 5'-AGTCGCACAAATCGTGTCTG-3' and reverse primer 5'-TCCATGCTCTCAGCATCAAC-3'. PCR reaction mixture includes single-stranded cDNA as a template, 0.4 µl of 10 µM forward and reverse primer, 0.4 µl of 10 mM dNTPs, 2 µl 10x buffer and 1.25 U of Opti*Taq* DNA polymerase (EURx, Poland) in the total volume of 20 µl. The thermal cycling conditions were as follows: 95°C for 30 s, 51°C (BnMT4) or 55°C (Bn5S) for 40 s, 72°C for 40 s for 26 cycles (Bn5S) or 28 cycles (BnMT4). PCR products were sequenced to confirm that specific fragments were amplified (Genomed, Poland). PCR products were separated on 2% agarose gels in TAE buffer with EtBr and their quantity was estimated by densitometric measurements using ImageGauge 3.46 software (FujiFilm, Japan).

Expression and purification of recombinant BnMT4 protein

The coding region for *BnMT4* was amplified by PCR on cDNA using sequence-specific primers containing *Nde*I and *Xho*I restriction sites: forward 5'-AAACATATGGCAGACATAGGCAAAGG-3' and reverse 5'-AAACTCGAGCTAAGCGGCACAAGAGGCG-3'. The PCR product was ligated with pET21a bacterial expression vector (Novagen, Germany) and the pET-*BnMT4* construct was checked by sequencing (GATC Biotech AG, Germany).

BnMT4 was overexpressed in *E. coli* Rosetta 2(DE3)pLysS (Novagen). Overnight cultures of transformed *E. coli* cells were diluted (1:100, *v/v*) with LB medium containing 50 µg/mL ampicillin and 34 µg/mL chloramphenicol. Protein expression was induced by 0.5 mM isopropyl-β-D-thiogalactopyranoside (IPTG) at an optical density at 600 nm (OD_{600}) of *ca.* 0.6-0.7 in the presence of either 0.5 mM $ZnSO_4$, 0.3 mM $CdSO_4$, or 0.1 mM $CuSO_4$. Bacteria were grown for a further 4-5 h at 37°C and harvested by centrifugation. Cell pellets were resuspended in sonication buffer (4 mL per gram of wet mass of cells; 50 mM Tris, 100 mM KCl, 3 mM DTT, 1 mM metal ion, 0.5% Trixton X-100, pH 8.5) and sonicated. The supernatant was separated from cell debris by centrifugation and was subjected to chemical precipitation with an ice-cold mixture of ethanol and chloroform (100:8, *v/v*).[50] Precipitated protein was dissolved in 20 mM NH_4HCO_3 buffer, filtrated (0.2 µm-0.4 µm, Minisart®) and purified by FPLC

(GE Healthcare Äkta Purifier, GE Healthcare, UK) using a size exclusion column (HiLoad 16/60 Superdex 75, Amersham Biosciences, UK) equilibrated with 20 mM NH_4HCO_3 buffer. The elution of the protein was monitored by measuring absorbance at 220 and 280 nm. All fractions were analysed for metal and sulfur content by inductively-coupled plasma optical emission spectroscopy (ICP-OES, Optima 5300 DV, Perkin-Elmer, UK; *vide infra*), and selected fractions were also analysed on SDS-PAGE gels. Proteins were resolved on precast 4–15% Mini-PROTEAN®TGX™ Gel (Bio-Rad, UK) in TGS (Tris/Glycine/SDS, pH 8.3; Bio-Rad) buffer and visualised by silver staining. Protein concentration was determined via measuring S content by ICP-OES or by measuring thiol content using Ellman's reaction[51] after demetallation by EDTA.

Elemental analysis

The contents of S, Zn, Cd and Cu in all samples were analysed by ICP-OES. Mixed-element calibration standards were prepared gravimetrically in the range of 0.2 – 5.0 ppm from commercial stocks (TraceCERT, Sigma-Aldrich). All samples and standards were prepared in 0.1 M HNO_3 (ultrapure 70% HNO_3 prepared in-house by sub-boiling point distillation).

Spectrometric and spectroscopic analysis of BnMT4

MT-containing fractions were pooled, desalted (Sephadex G-25, PD-10 desalting column, GE Healthcare) with 10 mM NH_4HCO_3 buffer and concentrated to 20-30 µM (Amicon Ultra-4 3000 Da MWCO) prior to analysis by electrospray ionisation (ESI) time-of-flight mass spectrometry (MicrOTOF, Bruker Daltonics, Germany). The parameters were as follows: temperature of ESI source: 468 K, mass spectral voltage parameters: 210 V – capillary exit, 450 V – hexapole RF, 1:70 V – skimmer, 1:19 V – hexapole. The samples in 10 mM NH_4HCO_3 and 10% MeOH were directly infused into the spectrometer by a syringe pump with a flow rate of 240 µL/h. Data were recorded for 2 min in positive mode over an m/z range of 500–3000. Spectra were averaged, smoothed and analysed using Data Analysis 4.0 software (Bruker Daltonics).

Proton-dependent loss of Zn(II) or Cd(II) ions bound to BnMT4 was analysed by UV-Vis spectroscopy using a Cary 50 Bio UV-Visible spectrophotometer (Varian, CA, USA) in the range of 200-400 nm at room temperature. The samples (7-10 µM in 1 mM Tris buffer pH 7.89) were placed in a quartz cuvette and were titrated with dilute HCl (0.05–0.5 M, ~1-2 µL) and UV-

spectra were recorded. The pH of the samples was measured using a benchtop meter (HANNA Instruments, UK) with BioTrode (Hamilton, NV, USA).

^{1}H NMR spectroscopy

For 1D and 2D ^{1}H NMR spectroscopy, Cd(II)-BnMT4 (950 µM) and Zn(II)-BnMT4 (880 µM) were prepared in 20 mM NH_4HCO_3 with 10% D_2O (*v/v*). NMR spectra were recorded at 298 K on a Bruker Avance 700 Ultrashield^{TM} spectrometer with a TCI cryoprobe operating at 700.24 MHz for ^{1}H. The Cd(II)-BnMT4 sample was titrated with microlitre additions of diluted HCl, and 1D ^{1}H NMR spectra were recorded between pH 8.09 and 3.07. 2D ^{1}H TOCSY and NOESY data were acquired for samples of Cd(II)-BnMT4 at pH 5.2 and Zn(II)-BnMT4 at pH 6.6, in each case at 298 K, with 4k datapoints in F2 and 512 datapoints in F1. Data were apodised using a shifted sinebell function, and Fourier-transformed with 2k×2k datapoints. In all cases, water suppression was achieved using excitation sculpting with gradients.[52]

Metal tolerance assays in bacteria

E. coli strain BL21(DE3) cells were transformed with an empty pET21a vector (control) or the pET-*BnMT4* construct. Overnight cultures of transformed *E. coli* were diluted (1:100, *v/v*) in LB medium supplemented with 50 µg/mL ampicillin, grown until OD_{600} reached *ca*. 0.6 and diluted again to OD_{600} *ca*. 0.2. At this point expression of BnMT4 protein was induced by IPTG at final concentrations of 0.1 or 0.3 mM, and metal ions were added to final concentrations of 0.25 or 0.5 mM of $ZnSO_4$, 0.1 or 0.25 mM of $CdSO_4$, and 0.075 or 0.165 mM of $CuSO_4$. Bacterial cells were collected every hour for seven hours, and the OD_{600} was measured. The growth rate of bacterial cultures, expressed as the slope of the linear proportion of the growth curve, was calculated using Microsoft Excel.

Statistical analyses

Statistical analyses were performed using PAST3.10 software.[53] ANOVA (analysis of variance) followed by Tukey's honestly significant difference test were used to determine significant differences between means. For the differences $p < 0.05$ (*) or $p < 0.01$ (**) was considered significant.

Results and discussion

Expression of BnMT4 during seed germination in the presence of heavy metal ions

The expression of MTs in several plant species is induced by metal ions;[21] however most of such studies have been limited to seedlings or vegetative parts of plants and thus only the expression of type 1-3 pMTs was examined.[54,55] Based on work demonstrating that during imbibition mRNA levels of E_c significantly increased in mature wheat embryos in the presence of abscisic acid (ABA) but not zinc,[27] it has been generally assumed that the expression of pMT4s is not influenced by metal ion levels. More recently, *AtMT4a* and *AtMT4b* expression was shown to be highly induced in ABA-treated siliques. Treatment with Zn did not change expression levels, but slight induction was observed after treatment with Cd;[17] therefore, metal-responsiveness of pMT4 genes is little studied, may differ between plant species and thus warrants investigation.

Germination is a crucial process in the life cycle of higher plants that determines all subsequent stages of growth and development and for crop plants also future yield; hence, we tested the effects of metals on the mRNA levels of *BnMT4* in germinating seeds of *B. napus* exposed to three heavy metals: cadmium, copper or zinc (Fig. 1). Transcripts of *BnMT4* in seeds germinating in water decreased during germination (Fig. 1) and were undetectable in 6-days-old seedlings.[30] The level of *BnMT4* mRNA appeared slightly increased (*ca*. 1.3-fold difference) in response to all three metals at the 3rd and 12th hour of imbibition; however, the differences were not statistically significant. During the subsequent 12 hours the *BnMT4* mRNA level remained unchanged in control and Cd-treated seeds and decreased in seeds exposed to Cu and Zn, but the difference was significant only for Cu-treated seeds – almost 3-fold lower than in the control. Between the first and second day of germination in seeds exposed to Cu, the mRNA level of *BnMT4* was marginally reduced, but remained high in seeds treated with Cd and Zn – 4.4- and 2.4-fold higher than that in the control, respectively. In Cd-treated seeds, no decrease in *BnMT4* expression was observed over the entire period while in the presence of Zn and Cu, the level of *BnMT4* transcript gradually decreased (Fig. 1).

In animals it was demonstrated that the metal-dependent upregulation of MT expression is mediated by metal-responsive elements (MREs) with a core sequence 5'-TGCRCNC-3', and the MRE-binding transcription factor-1 (MTF-1).[56] MRE-like sequences

have been identified in the promoters for type 1-3 pMTs,[57-59] but appear to be absent in the promoters of type 4 pMTs investigated so far. However, some novel putative regulatory elements mediating the response to metals have been identified in promoter regions of pMTs, e.g. in green algae,[60] bean,[61] rice[62-64] or oil palm.[65] *In silico* analysis of the putative promoter region of *BnMT4* using the PlantCARE database[66] revealed the presence of several regulatory elements, but none of them was related to heavy metals. However, manual analysis identified previously described plant-specific putative *cis*-elements conferring heavy-metal responsiveness (Supplementary Fig. S1). Therefore, it is possible that metal-ion responsive elements are present in the promoters of pMT4 genes. We also note that the observed effects may not necessarily result from de-novo gene expression, but could relate to differential stabilisation of already existing mRNA stored in the mature seeds.

Metal-binding capacity of the BnMT4 protein

The predicted amino acid sequence of BnMT4 shows highest similarity to sequences of MT4 from *Brassica oleracea* (XP_013627462.1) and *Brassica rapa* (XP_009134020.1), with 98% and 95% identities, respectively. Moreover, BnMT4 shares 79% identical amino acids with *Arabidopsis thaliana* MT4a (NP_001189730.1) and 80% with AtMT4b (NP_179905.1). Similarity to E_C-1 from monocotyledonous wheat is significantly lower (50% identities), but the number and positions of cysteine and histidine residues are fully conserved; this is, with very few exceptions, generally true for flowering plants (Fig. 2).[23]

Adopting the general approach pioneered by the Atrian and Capdevila team in Barcelona,[67] metal-to-protein stoichiometries of metal-BnMT4 complexes were analysed using recombinant BnMT4 protein (without any point mutations or artificial purification tags) produced in *E. coli* cultured in media supplemented with Cd(II), Cu(II) or Zn(II), respectively. After purification under conditions that preserve metal-MT complexes, metal contents were analysed using ICP-OES, and detailed qualitative metal speciation data were obtained using native ESI-MS (Table 1, Figs. 3, 4, Supplementary Fig. S2, Supplementary Tables S1, S2). The N-terminal methionine residue was in each case cleaved, a common feature for proteins synthesised in *E. coli*.[68] The molar Zn-to-protein ratio in purified Zn(II)-BnMT4 samples was 6.2 ± 0.5, with no other metals detected. The 6:1 stoichiometry was also corroborated by the predominant species observed in ESI-MS spectra at native pH. Its neutral mass of 8716.11 Da corresponds to Zn_6BnMT4 (Fig. 3A). In contrast, when BnMT4 was expressed in Cd- or Cu-

enriched media, significant amounts of Zn were also detected (Table 1). The molar Cd-to-BnMT4 ratio was 5.9 ± 0.5 (Table 1), in agreement with the predominant Cd_6BnMT4 species detected by ESI-MS (Fig. 3C). Consistent with the detection of 0.3 molar equivalents Zn(II) in the purified protein, ESI-MS spectra of Cd(II)-BnMT4 complexes also revealed the presence of Zn_1Cd_5BnMT4, together with minor quantities of seven- and eight-metal species (Fig. 3C). Acidification of Zn(II)- and Cd(II)-BnMT4 yielded the apo-form with a neutral mass of 8336.10 ± 0.35 Da (calculated 8467.54 Da for full-length protein and 8336.35 Da for protein with N-terminal methionine residue cleaved, cf. sequence in Fig. 2) as major species (Fig. 3B and D, respectively).

Generally, MTs incorporate copper in their Cu(I) oxidation state, as due to their redox potentials, Cu(II) and thiols cannot coexist. Moreover, in the reducing intracellular environment, copper is predominantly in its Cu(I) form. The intracellular copper content in *E. coli* is dependent on the level of culture aeration;[67] thus, the production of BnMT4 in Cu-enriched media was performed under both normal and reduced aeration conditions, following the example of Capdevila and Atrian.[69,70] ICP-OES results demonstrate that when BnMT4 was produced at normal aeration (low Cu(I)), heterometallic complexes containing 12.1 Cu and 1.4 Zn per BnMT4 were recovered. With reduced aeration (high Cu(I)), still heterometallic complexes were present (9.7 Cu and 0.7 Zn per BnMT4, respectively), but with a considerably higher copper-to-zinc ratio (Table 1): 13.9 *vs.* 8.6 under normal aeration. It is unknown why the overall metal-to-protein ratio was reduced under low aeration conditions. Mass spectra revealed that under both culture aeration conditions, BnMT4 expressed in the presence of Cu(I) yielded several coexisting metal-BnMT4 species at neutral pH (Fig. 4A, B). Although the presence of mixed-metallated species was suggested by ICP-OES results (Table 1), it is not possible in ESI-MS to unambiguously distinguish between Cu(I) and Zn(II) because of the small difference between their masses (taking into account the masses of protons to be formally replaced to maintain charge neutrality, the mass gain for one Zn(II) ion is 63.54, that for one Cu(I) ion 62.55). This ambiguity is further compounded by the possibility of thiol oxidation for under-metallated species, which results in lower than calculated masses. Significantly lower than expected masses were especially prevalent in samples synthesised under normal aeration conditions (Supplementary Table S2), i.e. with high levels of O_2 and hence less Cu(I) and more likelihood for oxidation. Only the Me_{14} species displayed a higher than calculated mass. ESI-MS spectra of Cu(I)-BnMT4 at acidic pH showed the presence of

several coexisting metallated species, but no apo-form (Fig. 4C). This is a common observation for Cu(I)-bound MT species and is owed to the high thermodynamic stability of Cu(I)-thiolate bonds.[71] Nevertheless, the reasonable agreement between calculated and observed masses for the Cu-bound species allows the conclusion that also in this case, the correct protein was isolated.

Besides wheat E_c-1, only a few other pMT4 proteins have been characterised. Recombinant *A. thaliana* MT4a and MT4b were shown to have the capacity to coordinate up to 6 Zn(II) and 6 Cd(II) ions, respectively.[23,72] The same metal stoichiometry was observed for *Helianthus annuus* MT4.[73] Recombinantly expressed MT4 from *Glycine max* (cv. Williams 82) bound 5-6 Zn(II) ions or 6 Cd(II) ions.[74] The lower Zn/protein stoichiometry is likely a consequence of this particular cultivar lacking the second, (normally) conserved His residue. Both His residues are required to form the mononuclear Zn(II) site, and the second His residue is critical for structuring the entire C-terminal domain.[48] Interestingly, for MT4 from *Sesamum indicum* and *Hordeum vulgare* expressed recombinantly in *E. coli*, unexpected poorly metallated complexes were observed – 2 Zn/SiMT4, 2 Cu/SiMT4[29] and 2.6 Zn/HvMT4, 0.19 Cu/HvMT4, 0.12 Cd/HvMT4,[32] respectively. The lower metal/MT ratios may not only be due to synthesis/purification approaches used but reflect the possible existence of partially metallated MT species *in planta*. In animals the existence of such species was confirmed, and their role as reactive oxygen species scavengers was suggested.[75] Moreover, it was proposed that (undermetallated) MTs may connect cellular redox balance and zinc metabolism.[76]

Traditional classification systems divide MTs into families based mainly on primary sequence similarities and phylogenetic relationships.[77,78] More recently, a classification system based on metal-binding properties of each MT peptide was proposed by the Barcelona team: a stepwise gradation between strict Zn- and genuine Cu-thioneins.[67,79] Although we consider pMT4s as prime examples of Zn-thioneins,[23,48,72] the occurrence of biologically relevant copper-MT4 interactions *in planta* cannot be excluded. Tarasava et al.[80] have shown recently that wheat E_C-1 binds copper in a site-specific manner *in vitro* and the possible existence of mixed-metal MT4 species *in planta* was suggested. E_C-1 protein isolated directly from wheat germs contained sub-stoichiometric amounts of copper[36] although it could not be ruled out that Cu(I) contamination occurred during purification. Nevertheless, the clean formation of the Zn_6BnMT4 species (Fig. 3A), contrasted with the observation of multiple heterometallic species when BnMT4 was produced in Cu-supplemented media (Fig. 4A and B,

Table 1), is consistent with the proposition that BnMT4, similarly to other pMT4s studied up to date, has clear Zn-thionein character.

pH stability of metal-BnMT4 complexes

The pH value of half-dissociation (pH(1/2)) is defined as the pH at which 50% of the initially bound metal ions have dissociated from the MT, and is typically measured by UV-Visible spectrophotometry, using the ligand-to-metal charge transfer (LMCT) bands at 230 nm (for Zn-MT, Fig. 5A) or 250 nm (for Cd-MT, Fig. 5B). The pH(1/2) is taken to correspond to the pH value of half-maximum absorbance $1/2(A_{max}+A_{min})$. This quantity is related to the protein's affinity towards the respective metal ion and is useful for comparing metal affinities of different MTs with each other.[81] Since Cd-S bonds are much stronger than Zn-S bonds, a higher proton concentration is required to displace Cd(II) ions from MTs compared to Zn(II), and hence pH(1/2) values for Cd-bound MTs are typically at least one pH unit lower than those for Zn-bound MTs.[71]

The pH(1/2) values for Zn_6BnMT4 and Cd_6BnMT4 complexes were estimated from plots of absorbance of the LMCT bands vs. the respective pH value (Fig. 5C, D). A value of 4.50 was obtained for Zn_6BnMT4 (Fig. 5C), similar to values obtained previously for Zn_6E_C-1 (4.53),[40] Zn_6AtMT4a (4.55) and Zn_6AtMT4b (4.56).[23] A value of 3.33 for Cd_6BnMT4 (Fig. 5D) is also almost identical to that of Cd_6E_C-1 (3.35),[40] and somewhat higher than the value of 3.1 obtained for both *Arabidopsis* MT4s.[23] As expected, both pH(1/2) and the pH at which the complete loss of initially bound metal ions occurs is significantly lower for Cd(II)-BnMT4 than for Zn(II)-BnMT4. However, loss of Cd(II) starts already at pH 7, indicating that some Cd(II) ions are bound quite weakly. There also appears to be a small additional step above pH 4. From the absorbance values at the start and end of the titration, it can be estimated that about 5 out of the *ca.* 6 Cd(II) ions are lost in the steep step.

The pH(1/2) values for Zn(II)- and Cd(II)-complexes of pMT4s are the lowest among pMTs, comparable to those of vertebrate MTs, which implies higher stability of metal-thiolate clusters.[22] Attempts to study BnMT4 synthesised in Cu-enriched media in the same way indicated that although a decrease of absorbance at 280 nm (LMCT band for Cu(I)) was observed (data not shown), complete release of metal ions was not achieved within accessible pH ranges, as observed previously by ESI-MS at acidic pH (Fig. 4C). Therefore, a pH(1/2) value could not be determined.

Proton-driven demetallation of Zn(II)- and Cd(II)-BnMT4 was further studied using ESI-MS which may inform about the fashion in which metallation/demetallation of MTs occurs (Fig. 6, Supplementary Tables S3 and S4).[82] The considerably different metal-binding behaviour of BnMT4 towards Zn(II) and Cd(II) is evident. Proton-dependent loss of Zn(II) ions occurs in a gradual fashion, with all possible species present during the pH titration (Fig. 6A-E). Zn_6BnMT4 was the most abundant species down to pH ~5 (Fig. 6A, B), with a significant amount of the Zn_5 species also observed at pH 5.05. Decrease of the pH value to 4.48 resulted in a mixture of all species ranging from Zn_1BnMT4 to Zn_6BnMT, with Zn_4BnMT4 being narrowly the most abundant (Fig. 6C). The apo-form was the predominant species detected at pH 4.14 (Fig. 6D) and 3.50 (Fig. 6E). The metal speciation determined by ESI-MS during the proton-dependent demetallation suggests that this occurs in a largely noncooperative fashion for Zn(II)-BnMT4, *i.e.* the loss of one metal ion does not affect the affinity to the remaining metal ions and thus, all partially metallated species have, apart from statistical effects, comparable Zn(II) affinity. Noncooperative demetallation was shown previously for Zn(II)-E_C-1 when reacted with EDTA,[83] although pH-dependent demetallation of Zn(II)-E_C led to the accumulation of a Zn_4E_C species, with virtually absent Zn_5E_C.[36] The comparable stabilities of partially metallated Zn-BnMT4 species highlights their potential for involvement in cellular Zn(II) chemistry.

In contrast, Cd_6BnMT4 (and also Cd_5Zn_1BnMT4 and Cd_7BnMT4) was stable against metal loss up to pH 5.4 (Fig. 6F, G). At pH 4.21 (Fig. 6H) a nearly equimolar mixture of Cd_5- and Cd_6BnMT4 complexes was detected. Interestingly, the Cd_5BnMT4 species was the major form observed down to pH 3.51 (Fig. 6I). The transition from Cd_5 to the apo-form occurred abruptly below this pH. At pH 3.06 the apo-form was the most abundant and only minor peaks corresponding to metallated species were observed (Fig. 6J). This abrupt loss is consistent with a certain degree of cooperativity within the Cd_5BnMT4 species. It is also noteworthy that this transition coincides with the steep drop in absorbance seen in the UV-Vis data (Fig. 5D), whereas the small drop in absorbance between pH 5 and 3.5 probably corresponds to the transition from Cd_6 to Cd_5.

The persistence of the Cd_5BnMT4 species observed by ESI-MS (Fig. 6F-J) is an intriguing unprecedented behaviour for pMT4 proteins. Therefore, ^{1}H NMR spectroscopy was used to further investigate metal-dependent protein folding.

^{1}H NMR spectroscopy: effect of metals on protein folding

The majority of zinc-MTs fold equally well with either Zn(II) or Cd(II), with the notable exception of wheat E_C-1.[48] To investigate whether the nature of the bound metal impacts protein folding in BnMT4, 2D TOCSY NMR spectra of Zn_6BnMT4 and Cd_6BnMT4 were acquired (Fig. 7). The appearance of the fingerprint region of the Zn_6BnMT4 spectrum is characteristic of a well-folded protein. This assessment is corroborated by partial sequential assignment. In contrast, Cd_6BnMT4 is only partially folded, as indicated by a lower number of dispersed backbone NH resonances, and an accumulation of NH resonances in the region typical of random-coil chemical shifts (ca. 8.0-8.5 ppm). In this case, partial sequential assignment reveals that the N-terminal γ-domain is well-folded, whereas the absence of assignable peaks for the C-terminal domain indicates structural disorder. This parallels observations made for wheat E_C-1;[37,48] the crucial role of the mononuclear Cys_2His_2 site in metal-dependent folding – and hence folding-mediated metal-discrimination – has been highlighted.[23,48] The underlying concept for this behaviour is Pearson's principle of hard and soft acids and bases:[84] The soft cation Cd(II) prefers the softer thiolate ligands of cysteines, whereas the borderline Zn(II) shows no clear preference for either histidine nitrogen or thiolate sulfur, as demonstrated previously.[85] Thus, the $ZnCys_2His_2$ site forms and promotes order in the C-terminal domain in the presence of Zn(II) only. The site does not form with Cd(II), which results in structural disorder.

Due to this behaviour, it has so far been impossible to derive a full experimental 3D structure for a pMT4, as this requires the determination of metal-to-ligand connectivities by heteronuclear [^{1}H,^{111}Cd] or [^{1}H,^{113}Cd] NMR experiments. ESI-MS data (Fig. 6F-J) imply a high relative stability of the Cd_5 species, and it was therefore of interest to explore whether this species was amenable to NMR structural studies. 1D ^{1}H NMR spectra were recorded at a range of pH values (Fig. 8), as inspection of dispersion and linewidths permits a quick assessment of overall folding. No dramatic changes in chemical shifts between pH 7.1 and 5.6 were observed, which implies that there was little to no change in protein folding. According to the ESI-MS data, the Cd_6 form dominates in this pH range. At pH 5.1 and below, the more dispersed resonances (e.g. those at 9.45, 8.95, 7.95, 7.80 ppm – belonging exclusively to the γ-domain) start decreasing in intensity, suggesting a loss of ordered structure in the γ-domain, too. The ESI-MS data indicate a transition from the Cd_6 to the Cd_5 form in this pH range, with the Cd_5 form dominating at pH 3.8-3.5. At pH 3, most NH backbone resonances are accumulated in a

broad unresolved fashion in the region expected for random coil chemical shifts, which indicates that the protein is now essentially unfolded (Fig. 8). In summary, it is likely that the Cd_5 species does not owe its persistence to a well-defined protein fold; in fact, it is likely that even the individual fold of the γ-domain may no longer be present in this metallospecies.

Metal ion tolerance of *E. coli* expressing BnMT4 protein

The ability of BnMT4 to incorporate Zn(II), Cd(II) and Cu(I) *in vivo* (in *E. coli*) was demonstrated earlier in this study. To establish whether such binding conferred tolerance against any of the metals tested, the effect of heterologous overexpression of BnMT4 on the growth of *E. coli* was investigated (Fig. 9). The addition of IPTG had a negative impact on growth irrespective of whether the cells were transformed with empty vector (pET21a) or pET-*BnMT4*. The similarity between these two results indicates that the protein itself is not toxic to *E. coli*. 0.5 mM Zn, and all concentrations of Cd or Cu also led to decreased growth, presumably due to metal toxicity. Any combination of IPTG and metal ion was also deleterious to bacterial growth, again irrespective of whether or not protein was expressed. A direct comparison between empty vector and pET-*BnMT4* under the same individual conditions reveals that there was no difference for growth in Cd-supplemented media. In the presence of Cu, there was a small decrease for pET-*BnMT4*, whereas only in the case of Zn, BnMT4 expression increased the growth rate. Notably, this effect was observed even in the absence of IPTG; it is suggested that this may be due to leaky expression, and indeed, this was confirmed by SDS-PAGE (Supplementary Fig. S3).

Thus, bacteria expressing BnMT4 showed increased tolerance only towards Zn whilst their tolerance towards Cd was not affected, and tolerance towards Cu was decreased in comparison to control cells expressing empty vector. Although increased tolerance of bacteria expressing other types of pMTs towards different metal ions was previously demonstrated,[86-88] heterologous expression of GST-AtMT4a and GST-AtMT4b did not enhance their tolerance towards Zn and Cu, but only led to higher cell contents of these two metals in bacterial cells.[17] AtMT4a and AtMT4b conferred higher Cu tolerance when expressed in the yeast mutant *Δcup1* and higher Zn tolerance and accumulation when expressed in a *Δzrc1Δcot1* mutant.[89] In contrast, a *Δace1* yeast mutant (ACE1 is a copper-dependent transcription factor responsible for activation of yeast metallothionein CUP1) overexpressing barley MT4 showed only slightly higher tolerance towards Cu, whereas no complementation was observed in case

of a cadmium-sensitive *Δycf1* strain, lacking a vacuolar GSH-conjugated cadmium transporter.[32] The *in planta* overexpression of *AtMT4a* and *AtMT4b* led to increased content of both Zn and Cu in seeds, but in *AtMT4a* and *ATMT4b* co-silencing lines, only the seed levels of Zn, but not Cu were reduced.[17] Ectopic expression of *AtMT4a* increased plants' tolerance towards Cu and Zn, but contrastingly only Cu accumulation was enhanced in vegetative tissues.[90]

The picture that emerges with respect to copper is that, when overexpressed in either *E. coli*, yeast, or in plants, type 4 MTs can contribute to copper binding and accumulation, but that this does not necessarily confer enhanced copper tolerance. This may be rationalised by considering that the MT4-bound Cu(I) may not be firmly sequestered by these proteins that have evolved to bind Zn(II), and as a consequence, Cu(I) may be released more readily and/or be redox-active when MT-bound. Furthermore, given the multitude of metallospecies formed, it is conceivable that these would be structurally disordered, as well-defined folds usually correlate with well-defined metal stoichiometry.[71] Such misfolded species are likely to be more prone to proteolysis, which would also result in release of Cu(I). In each of these scenarios, bacterial growth would be impaired due to copper toxicity (Fig. 9). We note that in plants and their seeds, there will be other proteins, including other pMTs, to ensure the safe handling of copper.

Conclusions

Summarily, the data presented in this study showed that

(i) the presence of metals during seed germination affected *BnMT4* mRNA levels (Fig. 1). The effect of copper differed from those of zinc and cadmium.

(ii) BnMT4 expressed in the presence of Cu forms a large range of mixed-metal (Cu and Zn) species (Fig. 4)

(iii) Cd_6-BnMT4, although the major metallospecies at neutral pH, is partially mis-folded (Figs. 3 and 7)

(iv) BnMT4 forms a well-defined Zn_6 species with a well-ordered protein fold (Figs. 3 and 7)

(v) BnMT4 overexpression in *E. coli* mitigated zinc toxicity, but did not confer tolerance towards either Cd or Cu (Fig. 9)

All observations are consistent with a role of BnMT4 in zinc homeostasis before and/or during germination. It is intriguing that despite the clearly demonstrated ability to strongly bind Cu and Cd, no tolerance to these metals was conferred to the heterologous host *E. coli*. We suggest that in both cases, this may be due to protein misfolding and enhanced degradation, with concomitant metal release. Based on these considerations, and particularly their dramatically different folding behaviour in the presence of Zn(II) vs. Cd(II), type 4 pMTs may act as metal-specificity filters. In this context, metal-dependent folding of BnMT4 may lead to preferential storage (in the maturing seed) of essential Zn over toxic Cd.

Acknowledgements

AMA's fellowship at the University of Warwick was supported by the European Union ("Enhancing Educational Potential of Nicolaus Copernicus University in the Disciplines of Mathematical and Natural Sciences" conducted under Sub-measure 4.1.1: Human Capital Operational Programme—Task 7 (Project No POKL.04.01.01-00-081/10)" and Marie Sklodowska-Curie Individual Fellowship conducted within Horizon2020 programme). AMA thanks Dr. Hasan Tanvir Imam for his support in laboratory work. We are grateful to the University of Warwick and Nicolaus Copernicus University for financial support and usage of facilities and we thank technical staff at the University of Warwick.

References

1 B. J. Alloway, Soil factors associated with zinc deficiency in crops and humans, *Environ. Geochem. Health*, 2009, **5**, 537-548.

2 C. Andreini, L. Banci, I. Bertini and A. Rosato, Zinc through the three domains of life, *J. Proteome Res.*, 2006, **5**, 3173-3178.

3 N. Roohani, Zinc and its importance for human health: an integrative review, *J. Research Med. Sci.*, 2013, **18**, 144-157.

4 E. Andresen, E. Peiter and H. Küpper, Trace metal metabolism in plants, *J. Exp. Bot.*, 2018, **69,** 909-954.

5 S. A. Sinclair and U. Krämer, The zinc homeostasis network of land plants, *Biochim. Biophys. Acta*, 2012, **1823**, 1553-15567.

6 Z. Rengel and R. D. Graham, Importance of seed zinc content for wheat growth on zinc deficient soil. I. Vegetative growth, *Plant Soil*, 1995, **173**, 259-266.

7 Z. Rengel and R. D. Graham, Importance of seed Zn content for wheat growth on Zn deficient soil. II. Grain yield, *Plant Soil*, 1995, **173**, 267-274.

8 H. S. Grewal and R. D. Graham, Seed zinc content influences early vegetative growth and zinc uptake in oilseed rape (*Brassica napus* and *Brassica juncea*) genotypes on zinc-deficient soil, *Plant Soil*, 1997, **192**, 191-197.

9 L. Ozturk, M. A. Yazici, C. Yucel, A. Torun, C. Cekic, A. Bagci, H. Ozkan, H. J. Braun, Z. Sayers and I. Cakmak, Concentration and localization of zinc during seed development and germination in wheat, *Physiol. Plant.*, 2006, **128**, 144–152.

10 E. Lombi, E. Smith, T. H. Hansen, D. Paterson, M. D. de Jonge, D. L. Howard, D. P. Persson, S. Husted, C. Ryan and J. K. Schjoerring, Megapixel imaging of (micro)nutrients in mature barley grains, *J. Exp. Bot.*, 2011, **62**, 273–228.

11 T. Iwai, M. Takahashi, K. Od, Y. Terada and K. T. Yoshida, Dynamic changes in the distribution of minerals in relation to phytic acid accumulation during rice seed development, *Plant Physiol.*, 2012, **160**, 2007–2014.

12 B. Ajiboye, I. Cakmak, D. Paterson, M. D. de Jonge, D. L. Howard, S. P. Stacey, A. A. Torun, N. Aydin and M. J. McLaughlin, X-ray fluorescence microscopy of zinc localization in wheat grains biofortified through foliar zinc applications at different growth stages under field conditions, *Plant Soil*, 2015, **392**, 357-370.

13 K. Eggert and N. von Wirén, Dynamics and partitioning of the ionome in seeds and germinating seedlings of winter oilseed rape, *Metallomics*, 2013, **5**, 1316-1325.

14 S. Clemens, Zn and Fe biofortification: the right chemical environment for human bioavailability, *Plant Sci.*, 2014, **225**, 52-57.

15 D. P. Persson, T. H. Hansen, K. H. Laursen, J. K. Schjoerring and S. Husted, Simultaneous iron, zinc, sulfur and phosphorus speciation analysis of barley grain tissues using SEC-ICP-MS and IP-ICP-MS, *Metallomics*, 2009, **1**, 418-426.

16 I. Kranner and L. E. Colville, Metals and seeds: biochemical and molecular implications and their significance for seed germination, *Environ. Exp. Bot*., 2011, **72**, 93–105.

17 Y. Ren, Y. Liu, H. Chen, G. Li, X. Zhang and J. Zhao, Type 4 metallothionein genes are involved in regulating Zn ion accumulation in late embryo and in controlling early seedling growth in *Arabidopsis*, *Plant, Cell Environ.*, 2012, **34**, 770-789.

18 Y. Kojima, P. A. Binz and J. H. R Kägi, in *Metallothionein IV*, ed. C. D. Klaassen, Birkhäuser Verlag AG, Basel, 1999, pp. 3-6.

19 C. A. Blindauer and O. I. Leszczyszyn, Metallothioneins: unparalleled diversity in structures and functions for metal ion homeostasis and more, *Nat. Prod. Rep.*, 2010, **27**, 720-741.

20 B. Lane, R. Kajioka and T. D. Kennedy, The wheat-germ E_c protein is a zinc-containing metallothionein, *Biochem. Cell Biol.*, 1987, **65**, 1001-1005.

21 C. S. Cobbett CS and P. Goldsbrough, Phytochelatins and metallothioneins: roles in heavy metal detoxification and homeostasis, *Annu. Rev. Plant Biol.*, 2002, **53**, 159-182.

22 E. Freisinger, Plant MTs – long neglected members of the metallothionein superfamily, *Dalton Trans*., 2008, **47**, 6663-6675.

23 O. I. Leszczyszyn, H. T. Imam and C. A. Blindauer, Diversity and distribution of plant metallothioneins: a review of structure, properties and functions, *Metallomics*, 2013, **5**, 1146-1169.

24 G. K. Zhou, Y. Xu, J. Li, L. Yang and J. Y. Liu, Molecular analyses of the metallothionein gene family in rice (*Oryza sativa* L), *J. Biochem. Mol. Biol.*, 2006, **39**, 595-606.

25 V. H. Hassinen, A. I. Tervahauta, H. Schat and S. O. Kärenlampi, Plant metallothioneins - metal chelators with ROS scavenging activity?, *Plant Biol.*, 2011, **13**, 225-232.

26 G. Dąbrowska, C. Baum, A. Trejgell and K. Hrynkiewicz, Impact of arbuscular mycorrhizal fungi on the growth and expression of gene encoding stress protein – metallothionein BnMT2 in the non-host crop *Brassica napus* L, *J. Plant Nutr. Soil Sci.*, 2014, **177**, 459-467.

27 I. Kawashima, T. D. Kennedy, T. Chino and B. G. Lane, Wheat E_c metallothionein genes. Like mammalian Zn^{2+} metallothionein genes, wheat Zn^{2+} metallothionein genes are conspicuously expressed during embryogenesis, *Eur. J. Biochem.*, 1992, **209**, 971-976.

28 W. J. Guo, W. Bundithya and P. B. Goldsbrough, Characterization of the *Arabidopsis* metallothionein gene family: tissue-specific expression and induction during senescence and in response to copper, *New Phytol.*, 2003, **159**, 369-381.

29 C. L. Chyan, T. T. Lee, C. P. Liu, Y. C. Yang, J. T. C. Tzen and W. M. Chou, Cloning and expression of a seed-specific metallothionein-like protein from sesame, *Biosci., Biotechnol., Biochem.,* 2005, **69**, 2319-2325.

30 G. Dąbrowska, A. Mierek-Adamska and A. Goc, Characteristics of *Brassica napus* L. metallothionein genes: expression in organs and during seed germination, *Aust. J. Crop Sci.*, 2013, **7**, 1324-1332.

31 M. Schiller, J. N. Hegelund, P. Pedas, T. Kichey, K. H. Laursen, S. Husted and J. K. Schjoerring, Barley metallothioneins differ in ontogenetic pattern and response to metals, *Plant, Cell Environ.*, 2014, **37**, 353-367.

32 J. N. Hegelund, M. Schiller, T. Kiche, T. H. Hansen, P. Pedas, S. Husted and J. K. Schjoerring**,** Barley metallothioneins: MT3 and MT4 are localized in the grain aleurone layer and show differential zinc binding, *Plant Physiol.*, 2012, **159**, 1125-1137.

33 G. K. Zhou, Y. F. Xu and J. Y. Liu, Characterization of a rice class II metallothionein gene: tissue expression patterns and induction in response to abiotic factors, *J. Plant Physiol.*, 2005, **162**, 686-696.

34 H. Collett, A. Shen, M. Gardner, J. M. Farrant, K. J. Denby and N. Illing, Towards transcript profiling of desiccation tolerance in *Xerophyta humilis*: construction of a normalized 11 k *X. humilis* cDNA set and microarray expression analysis of 424 cDNAs in response to dehydration, *Physiol. Plant.*, 2004, **122**, 39-53.

35 E. Freisinger, Structural features specific to plant metallothioneins, *JBIC, J. Biol. Inorg. Chem.*, 2011, **16**, 1035-1045.

36 O. I. Leszczyszyn, R. Schmid and C. A. Blindauer, Toward a property/function relationship for metallothioneins: histidine coordination and unusual cluster composition in a zinc-metallothionein from plants, *Proteins*, 2007, **68**, 922-935.

37 E. A. Peroza, R. Schmucki, P. Günter, E. Freisinger and O. Zerbe, The β_E-domain of wheat E_c-1 metallothionein: a metal-binding domain with a distinctive structure, *J. Mol. Biol.*, 2009a, **387**, 207-218.

38 J. Loebus, E. A. Peroza, N. Blüthgen, T. Fox, W. Meyer-Klaucke, O. Zerbe and E. Freisinger, Protein and metal cluster structure of the wheat metallothionein domain γ-E(c)-1: the second part of the puzzle, *JBIC, J. Biol. Inorg. Chem.*, 2011, **16**, 683-694.

39 E. A. Peroza and E. Freisinger, Metal ion binding properties of *Triticum aestivum* E_c-1 metallothionein: evidence supporting two separate metal thiolate clusters, *JBIC, J. Biol. Inorg. Chem.*, 2007, **12**, 377-391.

40 E. A. Peroza, A. Al Kaabi, W. Meyer-Klaucke, G. Wellenreuther and E. Freisinger, The two distinctive metal ion binding domains of the wheat metallothionein E_c-1, *J. Inorg. Biochem.*, 2009, **103**, 342-353.

41 V. Buchanan-Wollaston, Isolation of cDNA clones for genes that are expressed during leaf senescence in *Brassica napus*. Identification of a gene encoding a senescence-specific metallothionein-like protein, *Plant Physiol.,* 1994, **105**, 839-846.

42 C. Hanfrey, M. Fife and V. Buchanan-Wollaston, Leaf senescence in *Brassica napus*: expression of genes encoding pathogenesis-related proteins, *Plant Mol. Biol.*, 1996, **30**, 597-609.

43 V. Buchanan-Wollaston and C. Ainsworth, Leaf senescence in *Brassica napus*: cloning of senescence related genes by subtractive hybridisation, *Plant Mol. Biol*., 1997, **33,** 821-834.

44 H. M. Abdelmigid*,* Expression analysis of type 1 and 2 metallothionein genes in rapeseed (*Brassica napus* L.) during short-term stress using sqRT-PCR analysis, *Indian J. Exp. Biol*., 2016, **54**, 212-218.

45 Y. Pan, M. Zhu, S. Wang, G. Ma, X. Huang, C. Qiao, R. Wang, X. Xu, Y. Liang, K. Lu, J. Li, C. Qu, Genome-wide characterization and analysis of metallothionein family genes that function in metal stress tolerance in *Brassica napus* L. *Int. J. Mol. Sci*., 2018, **19**, 2181.

46 L. Tang, R. Qiu, Y. Tang and S. Wang, Cadmium-zinc exchange and their binary relationship in the structure of Zn-related proteins: a mini review, *Metallomics*, 2014, **6**, 1313-1323.

47 H. Küpper and E. Andresen, Mechanisms of metal toxicity in plants, *Metallomics*, 2016, **8,** 269-285.

48 O. I. Leszczyszyn, C. R. J. White and C. A. Blindauer, The isolated Cys_2His_2 site in E_c metallothionein mediates metal-specific protein folding, *Mol. BioSyst.*, 2010, **6**, 1592-1603.

49 R. F. Brennan and M. D. A. Bolland, Canola takes up more cadmium and phosphorus from soil than spring wheat, *J. Plant Nutr.*, 2005, **28**, 931-948.

50 M. Vašák, Large-scale preparation of metallothionein: biological sources, *Methods Enzymol.*, 1991, **205**, 39-41.

51 G. L. Ellman, Tissue sulfhydryl groups, *Arch. Biochem. Biophys.*, 1959, **82**, 70-77.

52 T. L. Hwang and A. J. Shaka, Water suppression that works. Excitation sculpting using arbitrary wave-forms and pulse-field gradients, *J. Magn. Reson., Ser. A*, 1995, **112**, 275-279.

53 O. Hammer, D. A. T. Harper and P. D. Ryan, PAST: paleontological statistics software package for education and data analysis, *Palaeo. Electron.*, 2001, **4**, pp9.

54 A. Kohler, D. Blaudez, M. Chalot and F. Martin, Cloning and expression of multiple metallothioneins from hybrid poplar, *New Phytol.*, 2004, **164**, 83-93.

55 Y. O. Ahn, S. H. Kim, J. Lee, H. Kim, H. S. Lee and S. S. Kwak, Three *Brassica rapa* metallothionein genes are differentially regulated under various stress conditions, *Mol. Biol. Rep*., 2012, **39**, 2059-2067.

56 G. W. Stuart, P. F. Searle and R. D. Palmiter, Identification of multiple metal regulatory elements in mouse metallothionein-I promoter by assaying synthetic sequences, *Nature*, 1985, **317**, 828-831.

57 I. M. Evans, L. N. Gatehouse, J. A. Gatehouse, N. J. Robinson and R. R. D. Croy, A gene from pea (*Pisum sativum* L.) with homology to metallothionein genes, *FEBS Lett*., 1990, **262**, 29-32.

58 C. A. Whitelaw, J. A. Le Huquet, D. A. Thurman and A. B. Tomsett, The isolation and characterization of the type II metallothionein-like genes from tomato (*Lycopersicon esculentum* L.), *Plant Mol. Biol.*, 1997, **33**, 503-511.

59 B. Usha, G. Venkataraman and A. Parida, Heavy metal and abiotic stress inducible metallothionein isoforms from *Prosopis juliflora* (SW) D.C. show differences in binding to heavy metals *in vitro*, *Mol. Genet. Genomics*, 2009, **281**, 99-108.

60 J. M. Quinn and S. Merchant, Two copper-responsive elements associated with the *Chlamydomonas Cyc6* gene function as targets for transcriptional activators, *Plant Cell*, 1995 **7,** 623-638.

61 X. Qi, Y. Zhang and T. Chai, Characterization of a novel plant promoter specifically induced by heavy metal and identification of the promoter regions conferring heavy metal responsiveness, *Plant Physiol*., 2007, **143**, 50-59.

62 Y. Ren and J. Zhao, Functional analysis of the rice metallothionein gene OsMT2b promoter in transgenic Arabidopsis plants and rice germinated embryos, *Plant Sci.*, 2009, **176**, 528–538.

63 C. J. Dong, Y. Wan, S. S. Yu and J. Y. Liu, Characterization of a novel rice metallothionein gene promoter: its tissue specificity and heavy metal responsiveness, *J. Integr. Plant Biol.*, 2010, **52**, 914-924.

64 G. Dąbrowska, A. Mierek-Adamska and A. Goc, Plant metallothioneins: putative functions identified by promoter analysis *in silico*, *Acta Biol. Cracov.*, 2012, **54**, 104-120.

65 V. Omidvar, S. N. A. Abdullah, A. Izadfard, C. L. Ho and M. Mahmood, The oil palm metallothionein promoter contains a novel AGTTAGG motif conferring its fruit-specific expression and is inducible by abiotic factors, *Planta*, 2010, **232**, 925-936.

66 V. Lescot, P. Dehais, G. Thijs, K. Marchal, Y. Moreau, Y. Van de Peer, P. Rouze and S. Rombauts, PlantCARE, a database of plant *cis*-acting regulatory elements and a portal to tools for *in silico* analysis of promoter sequences, *Nucleic Acids Res.*, 2002, **30,** 325–327.

67 O. Palacios, S. Atrian and M. Capdevila, Zn- and Cu-thioneins: a functional classification for metallothioneins?, *JBIC, J. Biol. Inorg. Chem.*, 2011, **16**, 991-1009.

68 P. H. Hirel, M. J. Schmitter, P. Dessen, G. Fayat and S. Blanquet, Extent of N-terminal methionine excision from *Escherichia coli* proteins is governed by the side-chain length of the penultimate amino acid, *Proc. Nat. Acad. Sci., USA*, 1989, **86**, 8247-8251.

69 J. Domènech, R. Orihuela, G. Mir, S. Atrian and M. Capdevila, The Cd(II)-binding abilities of recombinant *Quercus suber* metallothionein: bridging the gap between phytochelatins and metallothioneins, *JBIC, J. Biol. Inorg. Chem.*, 2007, **12**, 867-882.

70 R. Bofill, R. Orihuela, M. Romagosa, J. Domènech, S. Atrian and M Capdevila, *Caenorhabditis elegans* metallothionein isoform specificity - metal binding abilities and the role of histidine in CeMT1 and CeMT2, *FEBS J*., 2009, **276**, 7040-7056.

71 C. A. Blindauer, in *Binding, transport and storage of metal ions in biological cells*, ed. W. Maret and A. Wedd, Royal Soc. Chemistry, Cambridge, UK, 2014, pp. 606-665.

72 H. T. Imam and C. A. Blindauer, Differential reactivity of closely related zinc(II)-binding metallothioneins from the plant *Arabidopsis thaliana*, *JBIC, J. Biol. Inorg. Chem.*, 2018, **23**, 137-154.

73 M. Tomas, M. A. Pagani, C. S. Andreo, M. Capdevila, R. Bofill and S. Atrian, His-containing plant metallothioneins: comparative study of divalent metal-ion binding by plant MT3 and MT4 isoforms, *JBIC, J. Biol. Inorg. Chem.*, 2014, **19**, 1149-1164.

74 M. A. Pagani, M. Tomas, J. Carrillo, R. Bofill, M. Capdevila, S. Atrian and C. S. Andreo, The response of the different soybean metallothionein isoforms to cadmium intoxication, *J. Inorg. Biochem.*, 2012, **117**, 306-315.

75 W. Feng, F. W. Benz, J. Cai, W. M. Pierce and Y. J. Kang, Metallothionein disulfides are present in metallothionein-overexpressing transgenic mouse heart and increase under conditions of oxidative stress, *J. Biol. Chem.*, 2006, **13**, 681-687.

76 A. Krężel and W. Maret, Different redox states of metallothionein/thionein in biological tissue, *Biochem. J.*, 2007, **402**, 551-558.

77 N. J. Robinson, A. M. Tommey, C. Kuske and P. J. Jackson, Plant metallothioneins, *Biochem. J.*, 1993, **295**, 1-10.

78 P. A. Binz and J. H. R. Kägi, in *Metallothionein IV*, ed. C. D. Klaassen, Birkhäuser Verlag AG, Basel, 1999, pp. 7-13.

79 M. Valls, R. Bofill, R. González-Duarte, P. González-Duarte, M. Capdevila and S. Atrian, A new insight into metallothionein (MT) classification and evolution, *J. Biol. Chem.*, 2001, **276**, 32835-32843.

80 K. Tarasava, J. Loebus and E. Freisinger, Localization and spectroscopic analysis of the Cu(I) binding site in wheat metallothionein E_c-1, *Int. J. Mol. Sci*., 2016, **17**, E371.

81 E. Freisinger, in *Metal Ions in Life Sciences*, ed. A. Sigel, H. Sigel H and R. K. O. Sigel, Royal Soc. Chemistry, Cambridge, UK, 2009, vol. 5, pp. 107-153.

82 D. E. K. Sutherland and M. J. Stillman, The "magic numbers" of metallothionein, *Metallomics*, 2011, **3**, 444-463.

83 O. I. Leszczyszyn and C. A. Blindauer, Zinc transfer from the embryo-specific metallothionein E_c from wheat: a case study, *Phys. Chem. Chem. Phys.*, 2010, **12**, 13408-13418.

84 R. G. Pearson, Hard and soft acids and bases, *J. Am. Chem. Soc.*, 1963, **85**, 3533–3539.

85 B. A. Krizek, D. L. Merkle and J. M. Berg, Ligand variation and metal-ion binding-specificity in zinc finger peptides, *Inorg. Chem.*, 1993, **32**, 937-940.

86 A. Zhigang, L. Cuijie, Z. Yuangang, D. Yejie, A. Wachter, R. Gromes and T. Rausch, Expression of *BjMT2*, a metallothionein 2 from *Brassica juncea*, increases copper and cadmium tolerance in *Escherichia coli* and *Arabidopsis thaliana*, but inhibits root elongation in *Arabidopsis thaliana* seedlings, *J. Exp. Bot.*, 2006, **57**, 3575-3582.

87 Y. O. Kim, D. H. Patel, D. S. Lee, Y. Song and H. J. Bae, High cadmium-binding ability of a novel *Colocasia esculenta* metallothionein increases cadmium tolerance in *Escherichia coli* and tobacco, *Biosci., Biotechnol., Biochem*., 2011, **75**, 1912-1920.

88 E. Dundar, G. D. Sonmez and T. Unver, Isolation, molecular characterization and functional analysis of OeMT2, an olive metallothionein with a bioremediation potential, *Mol. Genet. Genomics*, 2015, **290**, 187-199.

89 W. J. Guo, M. Meetam and P. B. Goldsbrough, Examining the specific contributions of individual *Arabidopsis* metallothioneins to copper distribution and metal tolerance, *Plant Physiol.*, 2008, **146**, 1697-1706.

90 I. D. Rodríguez-Llorente, P. Pérez-Palacios, B. Doukkali, M. A. Caviedes and E. Pajuelo, Expression of the seed-specific metallothionein *mt4a* in plant vegetative tissues increases Cu and Zn tolerance, *Plant Sci.*, 2010, **178**, 327–332.

Table 1 Metal stoichiometry of recombinant BnMT4 protein determined by elemental analysis and major metal-MT species observed in ESI-MS. Me stands for Cu+Zn.

Supplemented metal	Zn/MT	Cd/MT	Cu/MT	Metal-MT species
Zn	6.2 ± 0.5	n.d.[a)]	n.d.	Zn_6
Cd	0.3 ± 0.2	5.9 ± 0.5	n.d.	Cd_6, Cd_5Zn_1
Cu (reduced aeration)	0.7 ± 0.4	n.d	9.7 ± 0.1	Me_{12} - Me_9
Cu (normal aeration)	1.4 ± 0.4	n.d	12.1 ± 0.5	Me_{14} - Me_8

[a)] n.d.: Levels were below the limit of detection

Fig. 1 Expression of rapeseed *BnMT4* in germinating seeds in response to metal treatment. Total RNAs were isolated from seeds after 3, 12, 24 and 48 hrs after the start of imbibition. Seeds treated with water (white bars) served as a control. The left-hand side shows relative expression levels expressed as the ratio of the densitometric measurement of the *bnMT4* RT-PCR product to the 5S rRNA RT-PCR product (*Bn5S*) (means from three independent experiments ± SE). Asterisks indicate significant differences (* $p < 0.05$, ** $p < 0.01$) between control and metal-treated seeds at a particular time point.

Fig. 2 Amino acid alignment of representative members of type 4 pMTs. Conserved cysteines are marked in bold. Histidine residues with potential metal-binding ability are highlighted in grey. The consensus sequences of Cys-rich domains were obtained through comparative analysis of numerous type 4 pMTs. GenBank accession numbers are as follows: BnMT4 *Brassica napus* (AFP57436.1, this study), TaMT4 (wheat E_c-1) *Triticum aestivum* (CAA48349.1), HvMT4 *Hordeum vulgare* (CAD88267.1), AhMT4 *Arachis hypogaea* (ABG57066.1), GmMT4b *Glycine max* (NP_001237409.2), AtMT4a *Arabidopsis thaliana* (NP_179905.1), BrMT4 *Brassica rapa* (XP_009134020.1), HaMT4 *Helianthus annuus* (XP_022016856.1), SiMT4 *Sesamum indicum* (AAG23841.1).

Fig. 3 Representative ESI-MS spectra (+6 charge state) of Zn-(A, B) and Cd-(C, D) BnMT4 at native pH (A, C) or acidic pH (B, D). Samples in 10 mM NH_4HCO_3, 10% MeOH, plus 2% formic acid for acidic pH samples. Likely Na^+ adducts are indicated with an asterisk, unknown contaminants are labelled with a hash. See Supplementary Table S1 for exact molecular masses.

Fig. 4 Representative ESI-MS spectra (+6 charge state) of Cu-BnMT4 at native pH (A, B) or acidic pH (C) synthesized at normal (A) or reduced (B) aeration level. Samples in 10 mM NH_4HCO_3, 10% MeOH, plus 2% formic acid for acidic pH samples. Me (C, D) stands for Zn+Cu. See Supplementary Table S2 for exact molecular masses.

Fig. 5 Proton-dependent loss of Zn(II) or Cd(II) bound to BnMT4. The upper panels show raw UV-Vis spectra of Zn_6BnMT4 (A) and Cd_6BnMT4 (B) at different pH values. (C) and (D) show plots of absorbance at either 230 nm for Zn(II)-thiolate LMCT bands (C) or 250 nm for Cd(II)-thiolate LMCT bands (D) against pH value. The lines in graphs C and D are drawn to guide the eye, and do not correspond to curve fits. The pH(1/2) values for Zn_6BnMT4 and Cd_6BnMT4 complexes were estimated by reading from the graphs (C, D) the pH value that corresponds to the ½(Amax + Amin). This figure is available in colour at *JXB online*.

Fig. 6 Speciation of Zn(II)- and Cd(II)-BnMT4 at different pH values (10 mM NH_4HCO_3, 10% MeOH) obtained by addition of dilute formic acid. Likely Na^+/K^+ adducts are indicated with an asterisk, the peak labelled with a hash is an unknown contaminant. See Supplementary Table S3 and Table S4 for exact molecular masses.

Fig. 7 Comparison of the fingerprint regions of 2D [^{1}H,^{1}H] TOCSY NMR spectra of Zn(II)-BnMT4 at pH 6.6 (black) and Cd(II)-BnMT4 at pH 5.2 (red). Samples (~ 0.9 mM) in 20 mM NH_4HCO_3 buffer and 10% D_2O. This figure is available in colour at *JXB online*.

Fig. 8 Overlay of the fingerprint region of 1D ^{1}H-NMR spectra of Cd_6BnMT4 acquired at different pH values. Samples (0.95 mM) in 20 mM NH_4HCO_3 and 10% D_2O. The strong triplet around 7 ppm visible at lower pH corresponds to the protons of the ammonium ion.

Fig. 9 Comparison of the growth of *E. coli* expressing BnMT4 (grey bars) with bacteria transformed with empty pET vector (white bars) in the presence of Zn(II), Cd(II) and Cu(II). The y axis corresponds to the slopes of bacterial growth curves that were obtained from plotting optical density against time. Media were supplemented with two different concentrations of metal ions and two concentrations of IPTG. Bacteria grown in medium without metals and with or without IPTG serve as a control (C). Data are means of three independent experiments ± SE. Asterisks indicate significant differences (* $p < 0.05$, ** $p < 0.01$) between control cells and cells expressing BnMT4 at particular conditions (metal and IPTG).

Fig. 1

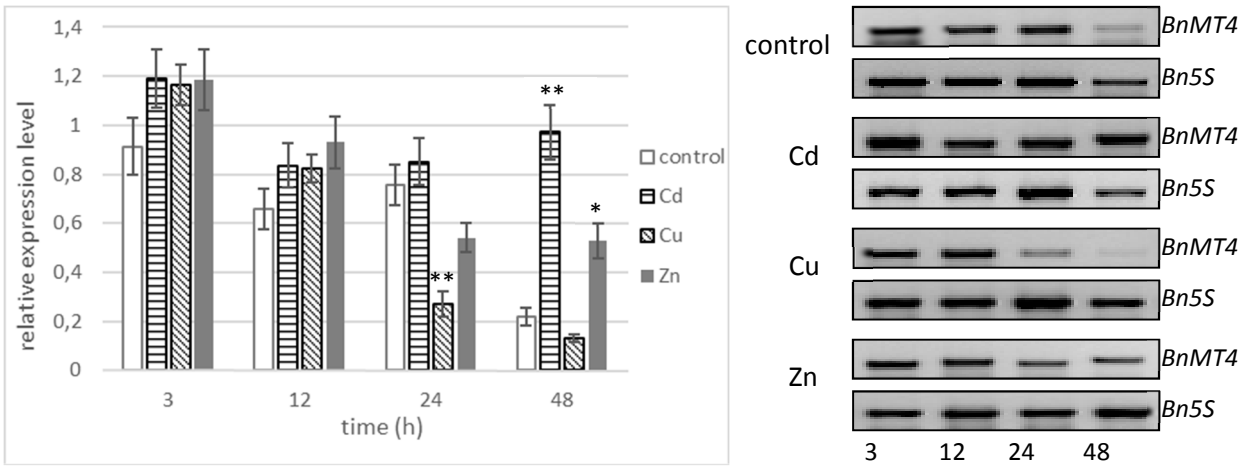
1,4
1,2
1
0,8
0,6
0,4
0,2
0
relative expression level
3
12
24
48
time (h)
control
Cd
Cu
Zn
**
**
*
control
Cd
Cu
Zn
BnMT4
Bn5S
BnMT4
Bn5S
BnMT4
Bn5S
BnMT4
Bn5S
3
12
24
48

Fig. 2

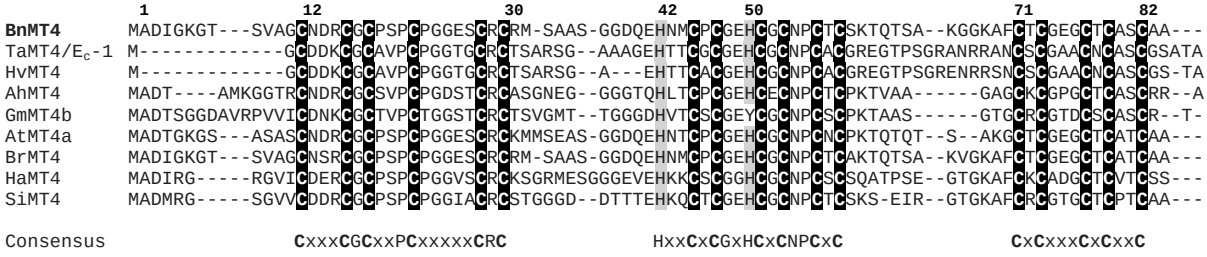
1
12
30
42
50
71
82
BnMT4 MADIGKGT---SVAGCNDRCGCPSPCPGGESCRCRM-SAAS-GGDQEHNMCPCGEHCGCNPCTCSKTQTSA--KGGKAFCTCGEGCTCASCAA---
TaMT4/Ec-1 M------------GCDDKCGCAVPCPGGTGCRCTSARSG--AAAGEHTTCGCGEHCGCNPCACGREGTPSGRANRRANCSCGAACNCASCGSATA
HvMT4 M------------GCDDKCGCAVPCPGGTGCRCTSARSG--A---EHTTCACGEHCGCNPCACGREGTPSGRENRRSNCSCGAACNCASCGS-TA
AhMT4 MADT----AMKGGTRCNDRCGCSVPCPGDSTCRCASGNEG--GGGTQHLTCPCGEHCECNPCTCPKTVAA------GAGCKCGPGCTCASCRR--A
GmMT4b MADTSGGDAVRPVVICDNKCGCTVPCTGGSTCRCTSVGMT--TGGGDHVTCSCGEYCGCNPCSCPKTAAS------GTGCRCGTDCSCASCR--T-
AtMT4a MADTGKGS---ASASCNDRCGCPSPCPGGESCRCKMMSEAS-GGDQEHNTCPCGEHCGCNPCNCPKTQTQT--S--AKGCTCGEGCTCATCAA---
BrMT4 MADIGKGT---SVAGCNSRCGCPSPCPGGESCRCRM-SAAS-GGDQEHNMCPCGEHCGCNPCTCAKTQTSA--KVGKAFCTCGEGCTCATCAA---
HaMT4 MADIRG-----RGVICDERCGCPSPCPGGVSCRCKSGRMESGGGEVEHKKCSCGGHCGCNPCSCSQATPSE--GTGKAFCKCADGCTCVTCSS---
SiMT4 MADMRG-----SGVVCDDRCGCPSPCPGGIACRCSTGGGD--DTTTEHKQCTCGEHCGCNPCTCSKS-EIR--GTGKAFCRCGTGCTCPTCAA---
Consensus CxxxCGCxxPCxxxxxCRC HxxCxCGxHCxCNPCxC CxCxxxCxCxxC

Fig. 3

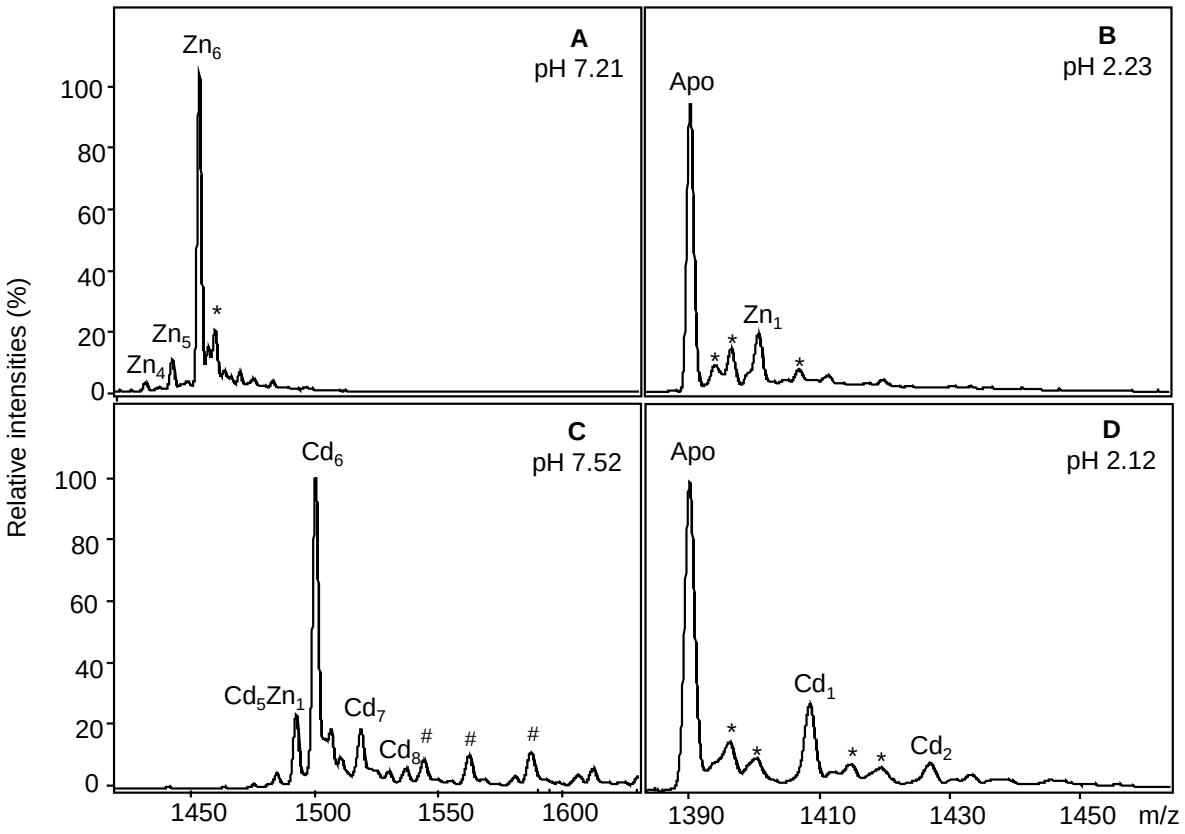
A
pH 7.21
Zn6
Zn5
Zn4
*
B
pH 2.23
Apo
Zn1
C
pH 7.52
Cd6
Cd5Zn1
Cd7
Cd8
#
D
pH 2.12
Apo
Cd1
Cd2
Relative intensities (%)
m/z
100
80
60
40
20
0
1450
1500
1550
1600
1390
1410
1430
1450

Fig. 4

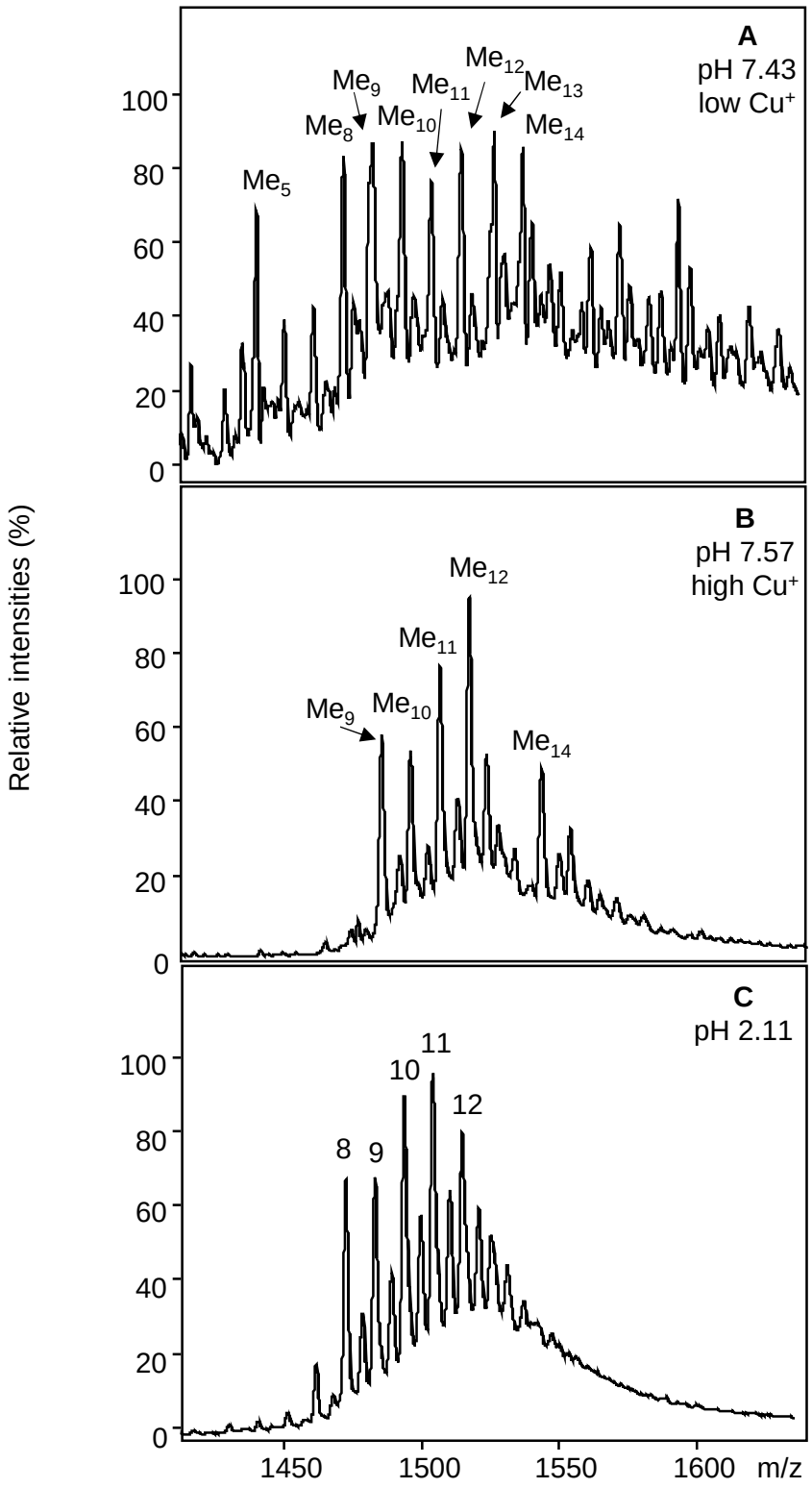
A
pH 7.43
low Cu+
Me5
Me8
Me9
Me10
Me11
Me12
Me13
Me14
B
pH 7.57
high Cu+
Me9
Me10
Me11
Me12
Me14
C
pH 2.11
8
9
10
11
12
Relative intensities (%)
0
20
40
60
80
100
1450
1500
1550
1600
m/z

Fig. 5

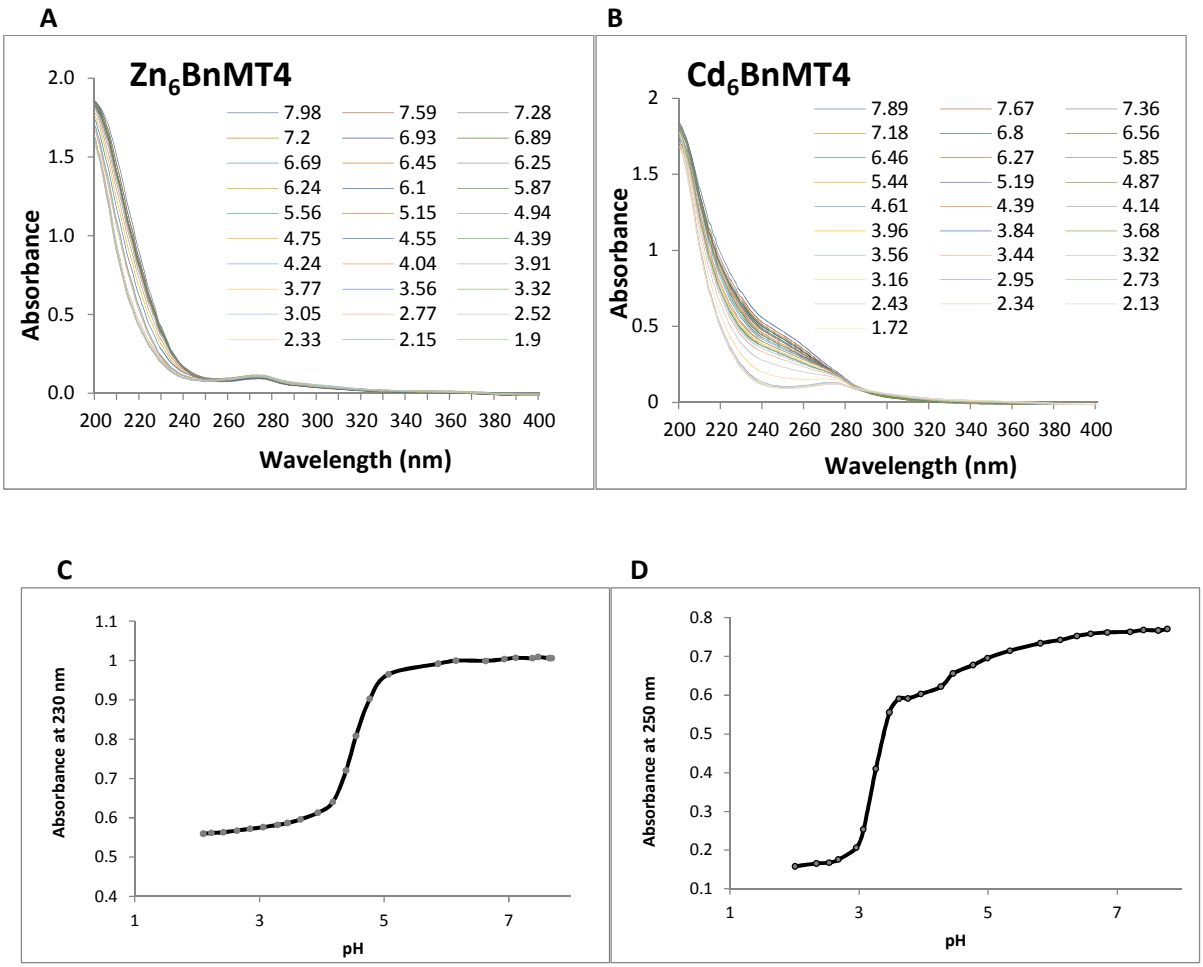
A
Zn6BnMT4
Absorbance
Wavelength (nm)
7.98 7.59 7.28
7.2 6.93 6.89
6.69 6.45 6.25
6.24 6.1 5.87
5.56 5.15 4.94
4.75 4.55 4.39
4.24 4.04 3.91
3.77 3.56 3.32
3.05 2.77 2.52
2.33 2.15 1.9
B
Cd6BnMT4
Absorbance
Wavelength (nm)
7.89 7.67 7.36
7.18 6.8 6.56
6.46 6.27 5.85
5.44 5.19 4.87
4.61 4.39 4.14
3.96 3.84 3.68
3.56 3.44 3.32
3.16 2.95 2.73
2.43 2.34 2.13
1.72
C
Absorbance at 230 nm
pH
D
Absorbance at 250 nm
pH

Fig. 6

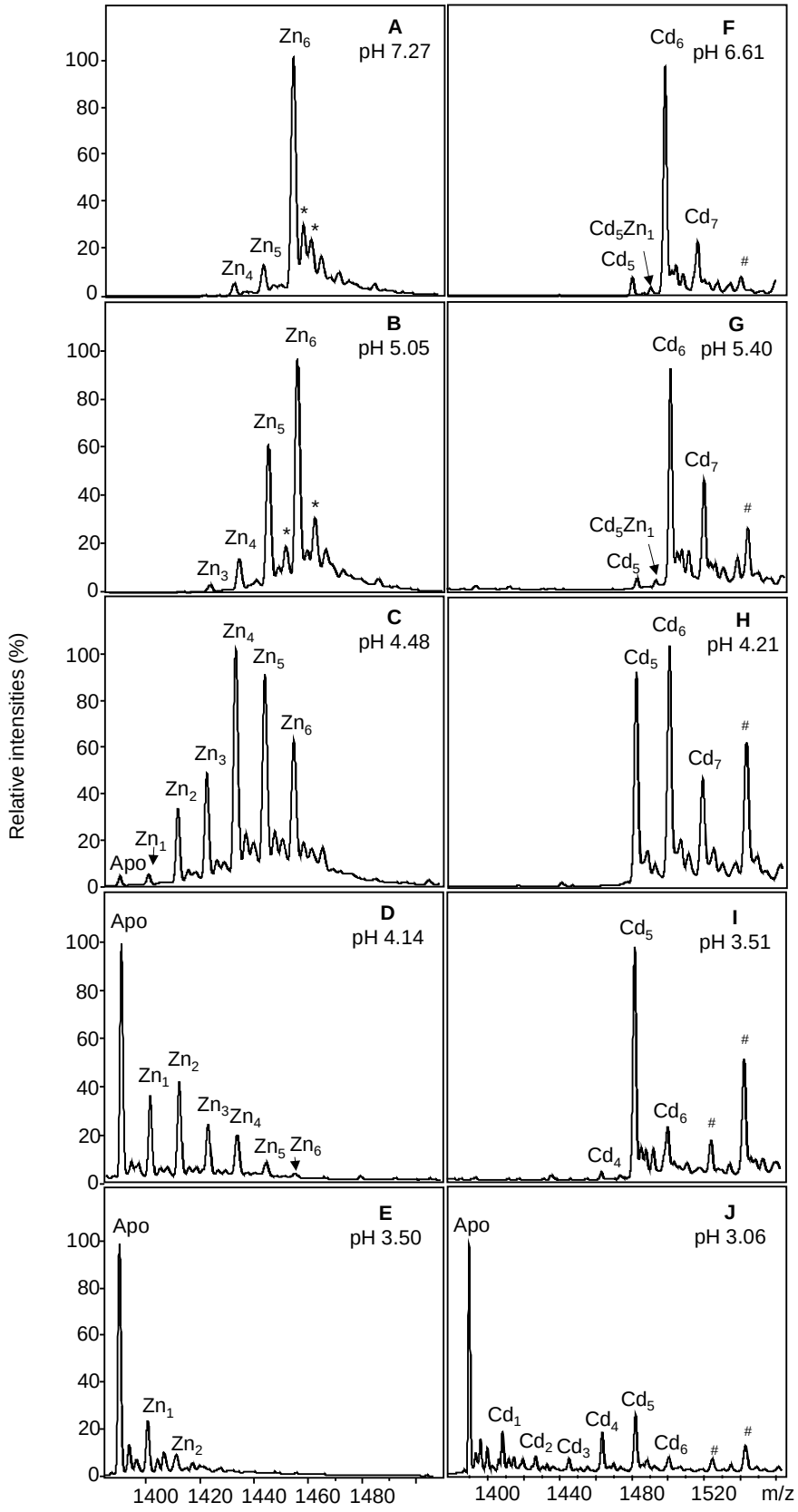
A
pH 7.27
Zn6
Zn5
Zn4
B
pH 5.05
Zn6
Zn5
Zn4
Zn3
C
pH 4.48
Zn4
Zn5
Zn6
Zn3
Zn2
Zn1
Apo
D
pH 4.14
Apo
Zn1
Zn2
Zn3
Zn4
Zn5
Zn6
E
pH 3.50
Apo
Zn1
Zn2
F
pH 6.61
Cd6
Cd5Zn1
Cd7
Cd5
G
pH 5.40
Cd6
Cd7
Cd5Zn1
Cd5
H
pH 4.21
Cd6
Cd5
Cd7
I
pH 3.51
Cd5
Cd6
Cd4
J
pH 3.06
Apo
Cd1
Cd2
Cd3
Cd4
Cd5
Cd6
Relative intensities (%)
1400 1420 1440 1460 1480
1400 1440 1480 1520 m/z

Fig. 7

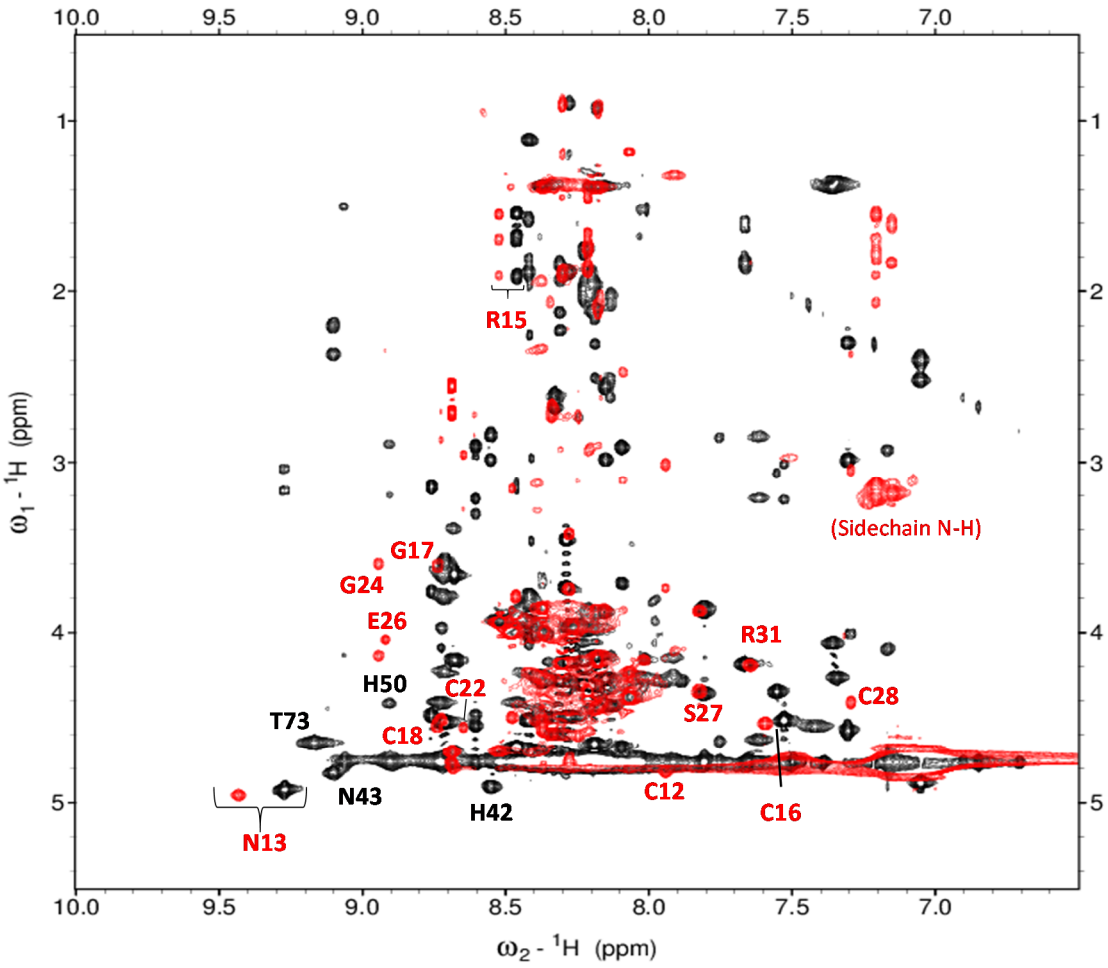
10.0
9.5
9.0
8.5
8.0
7.5
7.0
1
2
3
4
5
ω1 - 1H (ppm)
ω2 - 1H (ppm)
R15
(Sidechain N-H)
G17
G24
E26
R31
H50
C22
C28
S27
T73
C18
N43
H42
C12
C16
N13

Fig. 8

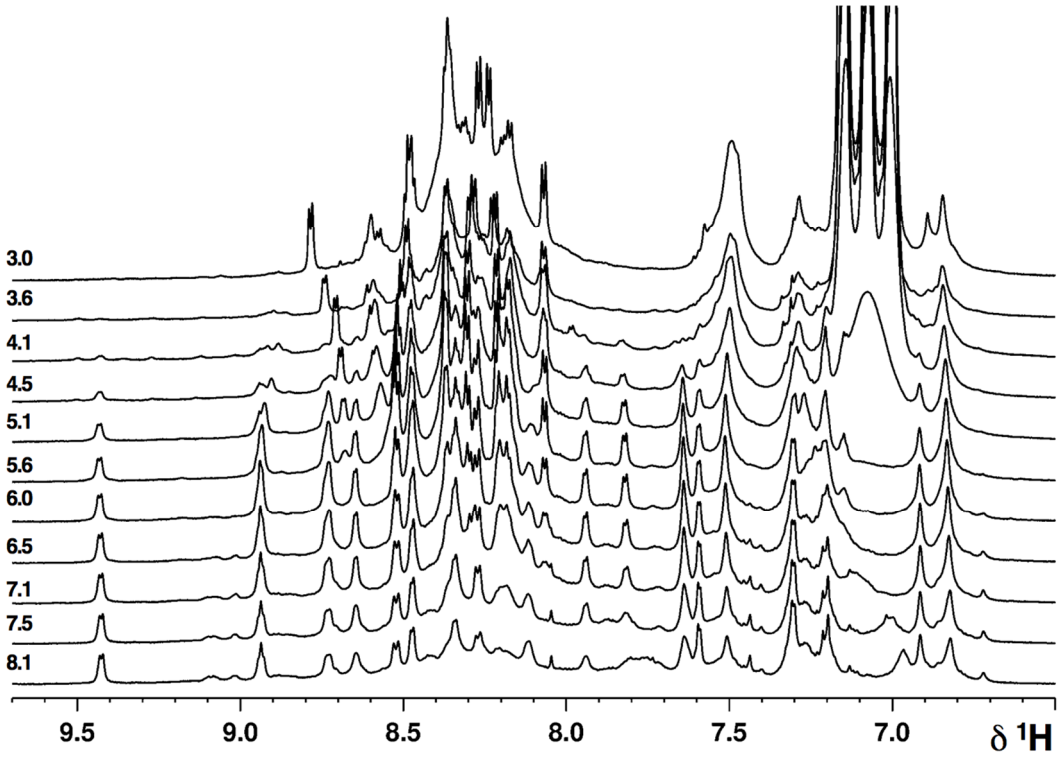

Fig. 9

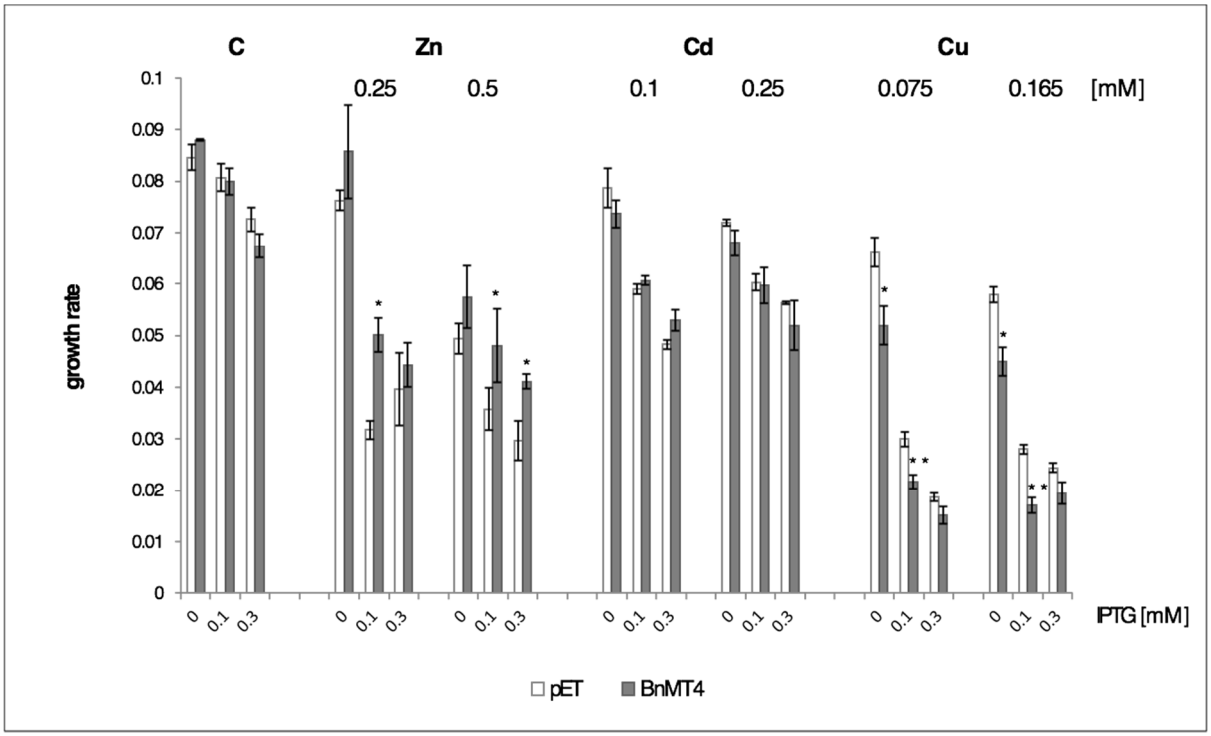
C
Zn
Cd
Cu
0.25
0.5
0.1
0.25
0.075
0.165
[mM]
growth rate
0.1
0.09
0.08
0.07
0.06
0.05
0.04
0.03
0.02
0.01
0
0
0.1
0.3
IPTG [mM]
pET
BnMT4